

Deformation and toughness of polymeric systems: 3. Influence of crosslink density

M. C. M. van der Sanden and H. E. H. Meijer*

Centre for Polymers and Composites (CPC), Eindhoven University of Technology,
PO Box 513, 5600 MB Eindhoven, The Netherlands
(Received 26 February 1993)

In part 1 of this series the phenomenon of a critical ligament thickness (ID_c) below which brittle polymers become ductile was investigated for polystyrene (PS). Using the thermoplastic polystyrene-poly(2,6-dimethyl-1,4-phenylene ether) (PS-PPE) model system, it was demonstrated in part 2 of this series that the absolute value of ID_c as well as the maximum toughness (i.e. maximum strain to break) was dependent on the network density of the polymer used. In this study the toughness and ID_c of crosslinked thermosetting polymers were investigated using epoxides based on the diglycidyl ether of bisphenol A as a model system. The crosslink density (v_c) is varied between values comparable with ($v_c = 9 \times 10^{25}$ chains m^{-3}), up to values much higher than ($v_c = 235 \times 10^{25}$ chains m^{-3}), the entanglement density in the thermoplastic PS-PPE system. The maximum macroscopic toughness proportional to the strain to break (λ_{macr}) or given by the slow-speed fracture toughness (G_c) and the notched high-speed tensile toughness (G_h) of core-shell rubber-modified epoxides uniquely increases with an increasing molecular weight between crosslinks (M_c). Only by using extreme testing conditions (notched high-speed impact testing), could the ID_c of a limited range of epoxides be determined: $0.21 \mu m$ ($v_c = 9 \times 10^{25}$ chains m^{-3}) $\leq ID_c \leq 0.29 \mu m$ ($v_c = 14 \times 10^{25}$ chains m^{-3}). Both the experimentally determined values of ID_c and the toughness of the epoxides compare well with the values determined for the entangled thermoplastic PS-PPE model system in the same range of network densities, elucidating the principal similarity of the influence of entanglements and crosslinks on the deformation processes. Good agreement was observed between the experimentally determined values of ID_c of the epoxides and the values predicted by the simple model introduced in part 2 of this series.

(Keywords: deformation; toughness; crosslink density)

INTRODUCTION

In our previous studies^{1,2} we have investigated the macroscopic toughness (strain to break) of neat and core-shell rubber-modified polystyrene and polystyrene-poly(2,6-dimethyl-1,4-phenylene ether) (PS-PPE) blends. Core-shell rubber-modified PS demonstrated the highest macroscopic draw ratio (λ_{macr}) within the investigated composition range: 3 (200%). Increasing the entanglement density (PPE content) of the matrix material resulted in a continuous decrease of λ_{macr} to a final value of 1.7 (70%). According to classical rubber elasticity theory³, the maximum draw ratio of a network (λ_{max}) is proportional to the molecular weight between entanglements (M_c):

$$\lambda_{max} \sim M_c^{1/2} \quad (1)$$

Comparing the experimentally determined values of λ_{macr} with the theoretical natural draw ratio of a network resulted in the following correlation:

$$\lambda_{macr}/\lambda_{max} = 0.6 \quad (2)$$

In order to obtain high strain values on a macroscopic level, the polymeric material had to be made very thin locally by the introduction of non-adhering rubbery particles ('holes'). The critical thickness below which the polymeric material demonstrates the maximum ductility

is called the critical ligament thickness (ID_c) and depends strongly on the network density². In part 2 of this series a simple model was presented that quantitatively describes the existence of ID_c based on an energy criterion². The available elastic energy (U_{av}) stored in a matrix ligament between two non-adhering rubbery particles is compared with the required surface energy (U_{re}) of a potential brittle fracture of the matrix ligament. Equating U_{av} with U_{re} resulted in an expression for ID_c dependence on several material parameters, i.e. network density (v ; entanglement and/or crosslink density), Young's modulus (E_1) and yield stress (σ_y) of the matrix material:

$$ID_c = \frac{6(\gamma + k_1 v^{1/2})E_1}{k_2 v^{-1/2} \sigma_y^2} \quad (3)$$

where γ is the van der Waals surface energy and k_1 and k_2 are constants ($k_1 = 7.13 \times 10^{-15}$ J chains^{-1/2} m^{-1/2} and $k_2 = 2.36 \times 10^{13}$ chains^{1/2} m^{-3/2})⁴.

In this study, the concept of a material specific ID_c is extended to thermosetting polymers. Compared with thermoplastic polymers, the class of thermosets comprises values of network density (crosslink density, v_c) comparable with, up to values much higher than, the entanglement density of most thermoplastic polymers: $9 \times 10^{25} \leq v_c \leq 250 \times 10^{25}$ chains m^{-3} . Hence, the theoretical maximum strain to break for this class of amorphous polymers is rather low compared with the

* To whom correspondence should be addressed

thermoplastic polymers, since the natural draw ratio is inversely proportional to the square root of the network density (see equation (1))³.

The thermosetting model system consists of epoxides based on the diglycidyl ether of bisphenol A (DGEBA), stoichiometrically cured with 4,4'-diaminodiphenyl sulfone (DDS). The macroscopic toughness was investigated not only by slow-speed uniaxial tensile testing but also by measuring the resistance to crack growth. For low testing rates (10 mm min⁻¹), the fracture toughness (G_{Ic}) was determined at room temperature. In order to investigate the toughness of the epoxides under very extreme testing conditions, notched high-speed (1 m s⁻¹) tensile tests were performed at various temperatures. The local thickness was set by changing the volume fraction of the previously introduced type of non-adhering core-shell rubbery particles¹. The ID_c data obtained from this study will be verified with predictions based on the simple first-order model introduced in our previous paper².

EXPERIMENTAL

Materials

Various epoxides were used, all based on the diglycidyl ether of bisphenol A (DGEBA, Epikote; Shell). Curing was performed using stoichiometric amounts of 4,4'-diaminodiphenyl sulfone (DDS; Aldrich). A non-adhering core-shell rubber with a poly(methyl methacrylate) shell and a styrene-butadiene core was used as impact modifier in concentrations of 5, 10, 15 and 20 wt% (Paraloid EXL 2600; powder form, produced by Rohm and Haas). The size of the rubbery particles was in the range 0.1–0.3 μm . Table 1 lists the properties of the epoxides.

Sample preparation

Neat epoxide resins were stirred mechanically with the DDS curing agent at different temperatures (see Table 2).

Table 1 Properties of Epikote as supplied by the Shell Chemical Co.

DGEBA type	Code	Epoxide equivalent weight (kg eq ⁻¹)	Physical appearance at room temperature
Epikote 1009	A	2.400–4.000 (3.200) ^a	solid
Epikote 1007	B	1.550–2.000 (1.775) ^a	solid
Epikote 1004	C	0.850–0.940 (0.895) ^a	solid
Epikote 1001	D	0.450–0.500 (0.475) ^a	solid
Epikote 828	E	0.182–0.194 (0.188) ^a	liquid

^a Average value of the epoxide equivalent weight (kg eq⁻¹), used to calculate the stoichiometric amount of DDS. The number-average molecular weight between crosslinks equals two times the epoxide equivalent weight in kg mol⁻¹.

Table 2 Preparation of neat and rubber-modified epoxide plaques

DGEBA type	Kneading step ^a		Mixing step		Curing step		Post-curing step	
	(°C)	(min)	(°C)	(min)	(°C)	(h)	(°C)	(h)
Epikote 1009	160	30	160	30	180	16	200	2
Epikote 1007	140	30	140	60	160	16	200	2
Epikote 1004	140	30	140	60	160	16	200	2
Epikote 1001	120	30	120	90	140	16	200	2
Epikote 828	120	30	120	45	120	16	220	2

^a Only in the presence of core-shell rubber

For the rubber-modified materials the epoxide resins were premixed with the core-shell rubber in a Brabender mixer (Model GNF 106/2), with the exception of the Epikote 828, which could be stirred mechanically because of its low viscosity at room temperature. After premixing, the DDS was added and the mixing was continued for at least 30 min (see Table 2: mixing step).

The blended materials were compression-moulded at a pressure of 40 MPa. Curing and post-curing were carried out according to Table 2.

Crosslink density

Two methods were used to determine the crosslink density (v_c) of the cured samples. The first method is based on the theory of rubber elasticity⁵. The number-average molecular weight between crosslinks (M_c) is correlated with the rubber plateau modulus (G_{No}):

$$M_c = \rho RT / G_{No} \quad (4)$$

where ρ is the density at temperature T and R is the universal gas constant⁵. Then v_c can be calculated using equation (4)⁴ since

$$v_c = \frac{\rho N_A}{M_c} \quad (5)$$

where N_A is Avogadro's number. G_{No} was measured using a Rheometrics RDSII dynamic mechanical spectrometer operated at an oscillating torsion frequency of 1 Hz. G_{No} is defined as the value of the storage shear modulus measured at 40°C above the glass transition temperature. Storage shear moduli were measured with a maximum strain amplitude ranging from 0.4 to 5% (0.4% in the glassy state and 5% in the rubbery region). The sample heating rate was 2°C min⁻¹ with a stabilization time of 1 min before measurement. All measurements were performed within the range 25 to 250°C using rectangular-shaped samples (50 mm × 12.5 mm × 2.9 mm).

The second method used to determine M_c of a crosslinked epoxide resin was based on an empirical relationship described by Nielsen⁶:

$$T_g - T_{go} = \frac{3.9 \times 10^4}{M_c} \quad (6)$$

where T_g is the glass transition temperature of the crosslinked epoxide resin and T_{go} is the glass transition temperature of the corresponding linear polymer. According to Bellenger *et al.*⁷ the value of T_{go} is 91°C for the DGEBA/DDS system. Glass transition temperatures were determined as being the maximum in $\tan \delta$, as obtained from dynamic mechanical data.

Mechanical properties

Strain to break. The post-cured samples were machined into dog-bone shaped tensile bars (DIN 53 455, sample thickness 7.5 mm) and then carefully polished using fine sand-paper to remove any irregularities introduced by the machining step. The polished samples were uniaxially strained on a Frank tensile machine (type: 81565 IV) at a crosshead speed of 5 mm min⁻¹ at room temperature. To ensure accurate data concerning the longitudinal strain level of the samples, extensometers were used. At least five specimens were fractured for each testing condition.

Fracture toughness. Fracture toughness (critical strain energy release rate; G_{Ic}) was measured according to the protocol of the European Group on Fracture of Polymers⁸. All measurements were performed on a single-edge notched (razor-blade tapped) three-point bending specimen. The specimens were machined to 50 mm × 10.35 mm × 7.5 mm (length × width × thickness). The span was approximately 42 mm. A crosshead rate of 10 mm min⁻¹ was used. All fracture toughness measurements were performed at room temperature using a Zwick hydraulic tensile machine (type Rel SB 3122). At least five specimens were fractured to obtain an average value of G_{Ic} .

Impact toughness. The high-speed notched impact toughness (G_h ; 1 m s⁻¹) is defined as the energy absorption during fracture of a single-edge notched (razor-blade tapped) tensile specimen divided by the original area behind the crack-tip of the specimen:

$$G_h = \frac{U}{t(w-a)} \quad (7)$$

where U is the absorbed energy during fracture (integrated area under the recorded stress-strain curve), t is the specimen thickness, w is the specimen width and a is the initial crack-length. The sample geometry was according to the Izod impact test protocol (ASTM D256). The specimen dimensions were: 55 mm × 12.5 mm × 2.9 mm. The free sample length between the clamps was 20 mm. All impact measurements were performed within the range -50 to +150°C on a Zwick Rel SB 3122 tensile machine equipped with a climate chamber. At least five specimens were fractured for each testing condition.

Microscopy

Scanning electron microscopy (SEM) was applied to investigate the morphology (i.e. homogeneity of the particle distribution) of the rubber-modified epoxides. Samples were fractured in liquid nitrogen and subsequently coated with an Au/Pd film. A Cambridge Stereo Scan 200 apparatus was used.

Visualization of the size of the whitened area (deformed region) of the fractured samples was carried out using reflection optical microscopy (ROM). After fracture, the specimens were embedded in a polyester matrix and polished to a thin sheet, perpendicular to the growth direction of the crack tip. Thin sections were then examined by reflected light.

RESULTS AND DISCUSSION

Crosslink density

In Figure 1 the storage shear modulus (G') and $\tan \delta$ of the stoichiometrically cured neat epoxide resins are plotted as a function of temperature. M_c is calculated from the rubber plateau modulus via equation (4) (see Table 3; a density of 1 g cm⁻³ is assumed).

For comparison, the M_c values determined from the glass transition temperature (equation (6)) are also listed in Table 3.

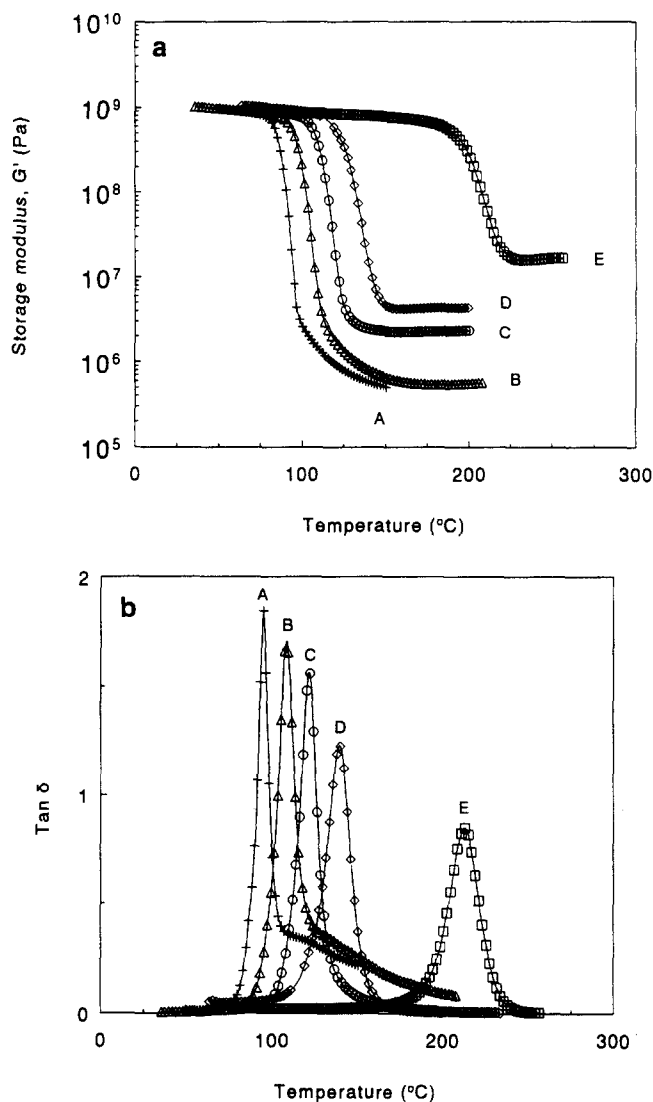


Figure 1 Dynamic mechanical data for neat epoxides: (a) storage modulus (G') versus temperature; (b) $\tan \delta$ versus temperature. The epoxide molecular weight between crosslinks: M_c = (A) 6.79; (B) 4.38; (C) 1.64; (D) 0.88; (E) 0.26 kg mol⁻¹

Table 3 Epoxide molecular weight between crosslinks

Code	Epoxide molecular weight (kg mol ⁻¹) ^a	M_c from G_{No} (kg mol ⁻¹)	T_g (°C)	M_c from T_g (kg mol ⁻¹)
A	4.80–8.00	6.79	95	9.30
B	3.10–4.00	4.38	109	2.23
C	1.70–1.88	1.64	122	1.25
D	0.90–1.00	0.88	140	0.80
E	0.36–0.39	0.26	213	0.32

^aData supplied by the manufacturer

The values of M_c obtained via the rubber elasticity theory agree well with the data of the epoxide monomer molecular weight supplied by the manufacturer (see Table 3). The values of M_c deduced from the empirical relationship described by Nielsen⁶ (equation (6)), on the other hand, demonstrate a deviation especially at high values of the epoxide monomer molecular weight. Clearly, the value of M_c increases with an increasing value of the epoxide monomer molecular weight. In the region of high values of the epoxide monomer molecular weight, the value of M_c cannot be set very accurately because of the small number of reactive epoxide groups per volume. In addition, the polydispersity of the epoxide system increases strongly at high values of the epoxide monomer molecular weight. Nevertheless, these materials are still suitable for the present investigation: M_c can be varied over a wide range; $0.26 \leq M_c \leq 6.79 \text{ kg mol}^{-1}$. Further in the discussion, only the M_c values obtained from G_{N_0} will be referred to. Table 4 lists the values for M_c and the crosslink density (ν_c ; see equation (5)) determined from G_{N_0} .

The epoxide having an M_c value of 6.79 kg mol^{-1} behaves like a real thermoplastic polymer as can be seen in Figure 1. The G' versus temperature curve does not clearly show a rubber plateau; instead, only a small change in slope is observed analogous to thermoplastics possessing a low molecular weight (see Figure 1, curve A). Also the $\tan \delta$ curve does not reach the value of zero after passing through the glass transition. The other epoxides clearly demonstrate a rubbery plateau after passing the glass transition temperature.

Morphology

As described in the experimental section, different volume fractions of non-adhering core-shell rubbers are added to the neat epoxide system. SEM was used to study the surfaces of liquid-nitrogen fractured samples in order to check the homogeneity of the particle distribution. Figure 2 shows two SEM micrographs of fracture surfaces of rubber-modified epoxides fractured in liquid nitrogen. It is clear that the rubber particle distribution is fairly homogeneous for both epoxides used despite the large differences in matrix viscosity.

Strain to break

The strain to break of the core-shell rubber-modified epoxides determined by uniaxial slow-speed tensile testing is shown in Figure 3.

The strain to break data for the neat epoxides are omitted because of the large scattering in these data caused by the high defect sensitivity of the samples. The epoxide with an M_c of 0.26 kg mol^{-1} is not analysed with respect to its slow-speed uniaxial tensile properties. In contrast with most core-shell rubber-modified PS-PPE blends^{1,2}, the strain to break of all of the rubber-modified

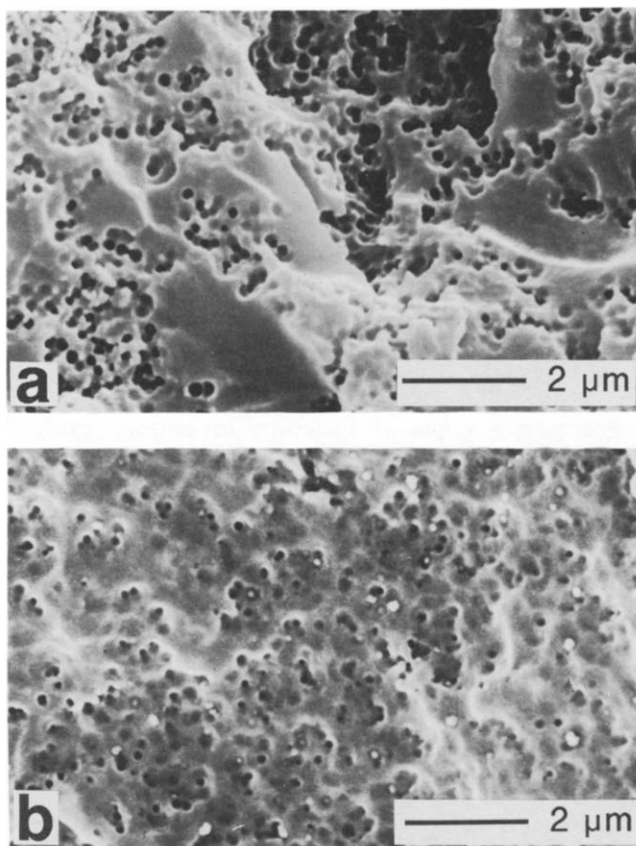


Figure 2 SEM micrographs of liquid-nitrogen fractured core-shell rubber-modified epoxides (10 wt%): (a) $M_c = 0.26 \text{ kg mol}^{-1}$; (b) $M_c = 6.79 \text{ kg mol}^{-1}$

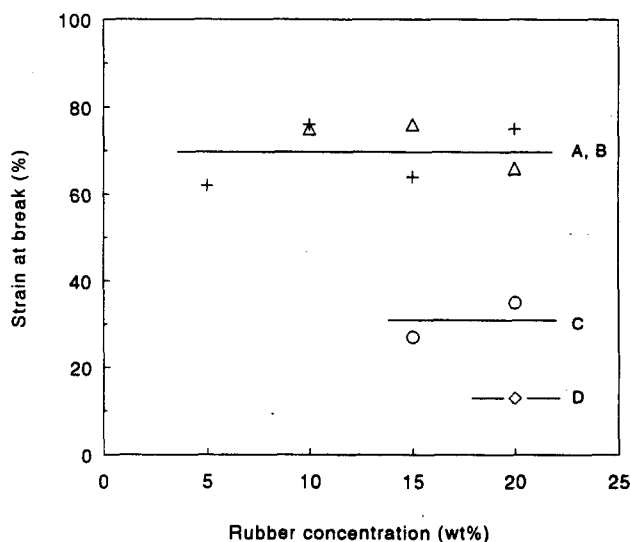


Figure 3 Strain at break of core-shell rubber-modified epoxides versus rubber concentration as a function of the epoxide molecular weight between crosslinks: $M_c =$ (A) 6.79; (B) 4.38; (C) 1.64; (D) 0.88 kg mol^{-1}

Table 4 M_c and ν_c determined from the rubber plateau modulus

DGEBA type	Code	M_c (kg mol^{-1})	ν_c (chains m^{-3})
Epikote 1009	A	6.79	9×10^{25}
Epikote 1007	B	4.38	14×10^{25}
Epikote 1004	C	1.64	37×10^{25}
Epikote 1001	D	0.88	68×10^{25}
Epikote 828	E	0.26	230×10^{25}

epoxides is constant, independent of the amount of core-shell rubber present. Clearly, no brittle-to-ductile transitions are detectable within the investigated range of testing speed and temperature. With an increasing M_c , the strain to break increases. Increasing the M_c of the epoxy matrix from 0.88 (curve D) to 6.79 kg mol^{-1} (curve A) leads to an increase in maximum strain to break from 12 to 70%. The maximum strain to break level of the epoxide with an M_c of 6.79 kg mol^{-1} agrees well with

that of a core-shell rubber-modified PS-PPE 20/80 blend ($M_c = 5.5 \text{ kg mol}^{-1}$, see ref. 2). In accordance with the findings here, this PS-PPE 20/80 w/w composition also did not show a brittle-to-ductile transition in uniaxial slow-speed tensile testing.

In Figure 4 the macroscopic draw ratio of core-shell rubber-modified epoxides is plotted versus the network density (filled circles). For comparison, the strain to break data for core-shell rubber-modified PS-PPE blends are incorporated in the same figure (open circles)^{1,2}.

The drawn line in Figure 4 (indicated by λ_{max}) is according to the maximum draw ratio of a single network strand (see equation (1)). As can be seen from Figure 4, the experimental data are all situated systematically below the drawn line. The dashed line, on the other hand, shows a close agreement with the experimentally determined (maximum) macroscopic draw ratios. The dashed line is according to equation (2), a relationship shown to be valid for the maximum macroscopic draw ratio of core-shell rubber-modified thermoplastic PS-PPE blends². Clearly, the experimental data obtained

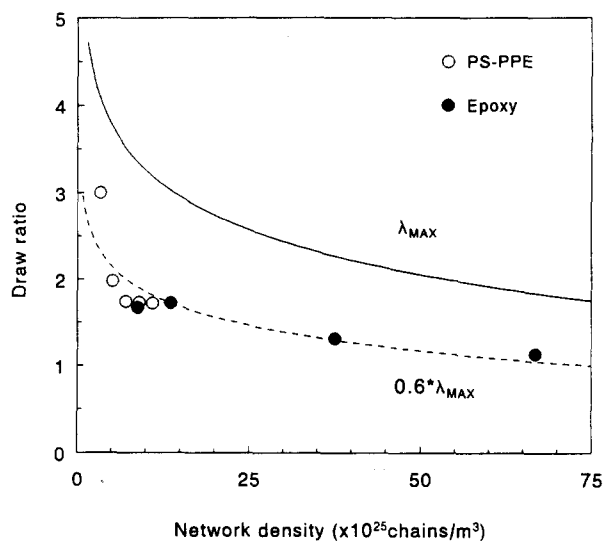


Figure 4 Draw ratio versus network density (entanglement and/or crosslink density). See text for details

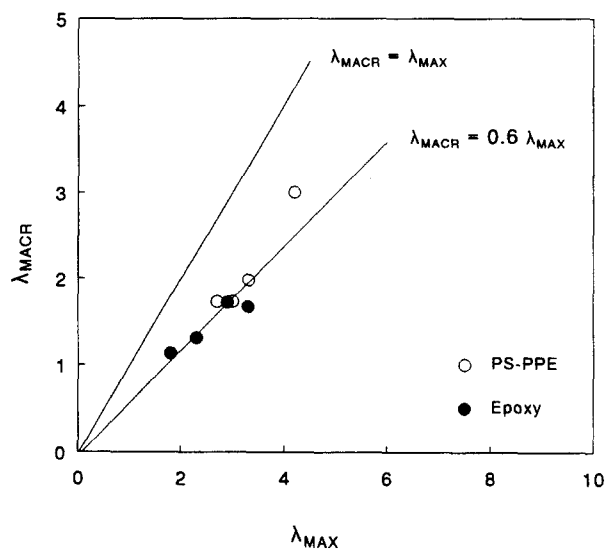


Figure 5 Maximum macroscopic draw ratio (λ_{MACR}) versus the natural draw ratio (λ_{MAX}) for core-shell rubber-modified epoxides and thermoplastic PS-PPE blends

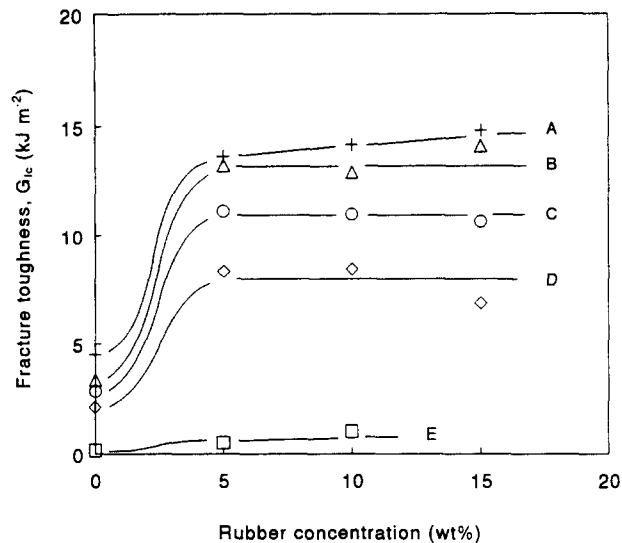


Figure 6 G_{1c} fracture toughness versus rubber concentration for neat and rubber-modified epoxides as a function of the epoxide molecular weight between crosslinks: M_c =(A) 6.79; (B) 4.38; (C) 1.64; (D) 0.88; (E) 0.26 kg mol^{-1}

from the crosslinked epoxides coincide with the dashed line. The physical origin of the lower value found for the maximum attainable macroscopic strain to break is related to the difference between the idealization of a representative single network strand and a fully three-dimensional structure of strands with a distribution in molecular weight between network nodes^{1,2,4,9}.

Figure 5 confirms the statements made above; the maximum macroscopic draw ratio is plotted versus the theoretical natural draw ratio, λ_{max} . The data obtained from the core-shell rubber-modified epoxides show some overlap with the data extracted from the thermoplastic PS-PPE system^{1,2}, clearly demonstrating the principal similarity of the influence of a chemical crosslink- and a physical entanglement-network on the deformation behaviour of polymer systems.

Fracture toughness

As mentioned, the low-entangled thermoplastic PS-PPE blends already show a brittle-to-ductile transition with increasing core-shell rubber content in slow-speed tensile testing at room temperature. For the PS-PPE 20/80 w/w composition, more extreme testing conditions are needed, e.g. notched tensile testing at high speed and/or low temperature¹⁰. (For a more detailed analysis of the influence of testing speed and temperature on the value of the critical ligament thickness of thermoplastic PS-PPE systems the reader is referred to part 4 of this series¹⁰). By definition, the critical ligament thickness is the material specific thickness below which the polymer network can be stretched to its theoretical extension ratio. Hence, in order to obtain more information on thermosets concerning the phenomenon of a brittle-to-ductile transition in relation to a critical ligament thickness between rubbery particles, the mode-I fracture toughness and high-speed tensile toughness of neat and core-shell rubber-modified epoxides was investigated. In Figure 6, the G_{1c} fracture toughness data for the neat and rubber-toughened epoxides are shown as a function of the epoxide monomer molecular weight (M_c).

The G_{1c} of the neat epoxides (0 wt% rubber) is rather sensitive towards changes in M_c ; G_{1c} increases from 0.15 kJ m^{-2} ($M_c = 0.26 \text{ kg mol}^{-1}$) to approximately 4.5 kJ m^{-2} ($M_c = 6.79 \text{ kg mol}^{-1}$). The latter G_{1c} value is still within the validity limits of the G_{1c} test. Comparing the G_{1c} data of the neat epoxides with data published by Pearson and Yee¹¹, it can be concluded that our G_{1c} values are considerably higher than those listed in ref. 11. This may be due to differences in the M_c values; Pearson and Yee used molecular weights in the range $0.34\text{--}3.6 \text{ kg mol}^{-1}$ while in this investigation up to 6.8 kg mol^{-1} was used. The rather high G_{1c} values of the neat epoxides could also partly originate from plastic deformation occurring at the crack tip. It would be more convenient to compare the G_{1c} value of the epoxide with an M_c value of 6.79 kg mol^{-1} with toughness data of neat thermoplastics having a molecular weight between entanglements of approximately 6.5 kg mol^{-1} . This topic will be discussed in more detail in a forthcoming paper¹⁰.

Adding 5 wt% core-shell rubbery particles to the epoxides results in a strong increase in fracture toughness, except for the epoxide having the lowest M_c (0.26 kg mol^{-1}). Further increasing the rubber concentration does not result in a further increase in G_{1c} . Although the G_{1c} values of the core-shell rubber-modified epoxides do not meet the requirements imposed by the validity criteria of the protocol of the European Group on Fracture of Polymers⁸, a quantitative comparison can still be made between the various rubber-modified epoxides. Clearly, the fracture toughness value of the rubber-modified epoxides depends on the epoxide monomer molecular weight: G_{1c} increases from 0.4 kJ m^{-2} ($M_c = 0.26 \text{ kg mol}^{-1}$; 5 wt% rubber) to 14 kJ m^{-2} ($M_c = 6.79 \text{ kg mol}^{-1}$; 5 wt% rubber). Hence, the fracture toughness values of the core-shell rubber-modified epoxides display the same trend as already observed for the maximum strain to break of these materials (compare Figure 3), confirming the statement that toughness is mainly dictated by the strain to break and to a lesser extent by the yield stress¹.

Clearly, a brittle-to-ductile transition is observed between 0 and 5 wt% core-shell rubber for all the epoxides shown in Figure 6 (excluding the epoxide with an M_c value of 0.26 kg mol^{-1}). However, the exact determination of the ID_c cannot be done. The calculated ID_c is located between $0.35 \mu\text{m}$ (based on 5 vol% rubbery particles having a diameter of $0.2 \mu\text{m}$ and assuming a body-centred lattice^{12,13}) and infinity. Moreover, no distinction can be made between the ID_c values for the various epoxides, so no M_c dependence can be extracted from these experiments. In order to determine the values of the ID_c more accurately, small-weight fractions ($\approx 0.5\text{--}5 \text{ wt}\%$) of larger (non-adhering to the matrix) rubbery particles should be used or more extreme testing conditions should be chosen (e.g. notched high-speed impact testing at low temperatures).

Impact toughness

For the semi-crystalline thermoplastic system polyamide-6/(easy cavitating) rubber, Borggreve *et al.*^{13,14} have shown that a brittle-to-ductile transition can be observed not only as a consequence of a change in matrix ligament thickness but also by increasing the testing temperature at a constant value of the matrix ligament thickness. The authors^{13,14} have also shown that the temperature at which the brittle-to-ductile transition occurred was independent of the glass transition temperature of the

matrix and of the dispersed rubbery phase. Because brittle-to-ductile transitions for the epoxides studied in this investigation are not observed during slow-speed uniaxial tensile testing and cannot be very accurately analysed with respect to their M_c dependence using (slow-speed) fracture toughness measurements, notched high-speed tensile toughness (G_h) measurements were performed within the temperature range -50 to 150°C . In Figure 7 the G_h values of the neat and rubber modified epoxides are displayed as a function of testing temperature.

Figure 7a shows that the neat epoxides demonstrate brittle fracture behaviour over the entire temperature range investigated. Although there is some scattering in the data, there seems to be no correlation between the epoxide monomer molecular weight and the energy absorption.

If 5 wt% core-shell rubber is added, the energy absorption during fast tensile fracture depends strongly on both the testing temperature and the epoxide monomer molecular weight (see Figure 7b). The highly crosslinked epoxides (curves D and E, $M_c = 0.88$ and 0.26 kg mol^{-1} , respectively) still behave 'brittle' at temperatures up to 150°C . The epoxides corresponding to curves A, B and C ($M_c = 6.79$, 4.38 and 1.64 kg mol^{-1} , respectively) already demonstrate the characteristics of a brittle-to-ductile transition with increasing temperature. The epoxide with an M_c of 4.38 kg mol^{-1} (curve B) possesses the most pronounced transition with increasing temperature. Clearly, the brittle-to-tough transition temperature (T_{BT}) is located at 35°C for this epoxide with a ligament thickness of $0.35 \mu\text{m}$ (corresponding to 5 wt% core-shell rubber). Surprisingly, the epoxide having the highest M_c (curve A) does not possess the highest degree of ductility. Apparently, for this epoxide the ID_c is not yet reached under the given testing conditions within the temperature range investigated, with the addition of 5 wt% rubber.

If the concentration of the core-shell rubber is raised to 10 wt%, stronger dependencies of G_h on M_c are observed, as shown in Figure 7c. The epoxides having a densely crosslinked network structure (curves C, D and E) still respond in a brittle manner over the entire temperature range investigated, analogous to the 5 wt% core-shell rubber-modified epoxides (compare Figures 7b and 7c). The epoxide having an M_c of 4.38 kg mol^{-1} (curve B), on the other hand, shows a pronounced increase in ductility compared to the 5 wt% rubber-modified epoxide; the maximum level of toughness, G_h , is increased and the brittle-to-ductile transition temperature is lowered by 15°C . Hence, the ID_c of this epoxide is located at $0.24 \mu\text{m}$ (corresponding to 10 wt% rubber) at 15°C under the given circumstances. The epoxide corresponding to curve A demonstrates a strong increase in ductility due to the increased rubber concentration (compare curve A in Figures 7b and 7c) and a sharp transition is observed at 30°C .

Further increasing the rubber concentration to 15 wt% confirms the trends as described above; see Figure 7d. The tensile toughness of epoxides corresponding to curves C and D (epoxide E is omitted for the sake of simplicity) is not influenced by an increase in rubber concentration. Also, the maximum level of tensile toughness of the epoxide with an M_c of 4.38 kg mol^{-1} (curve B) remains unchanged; only the value of T_{BT} is decreased by an extra 5°C compared to the 10 wt% rubber-modified epoxide.

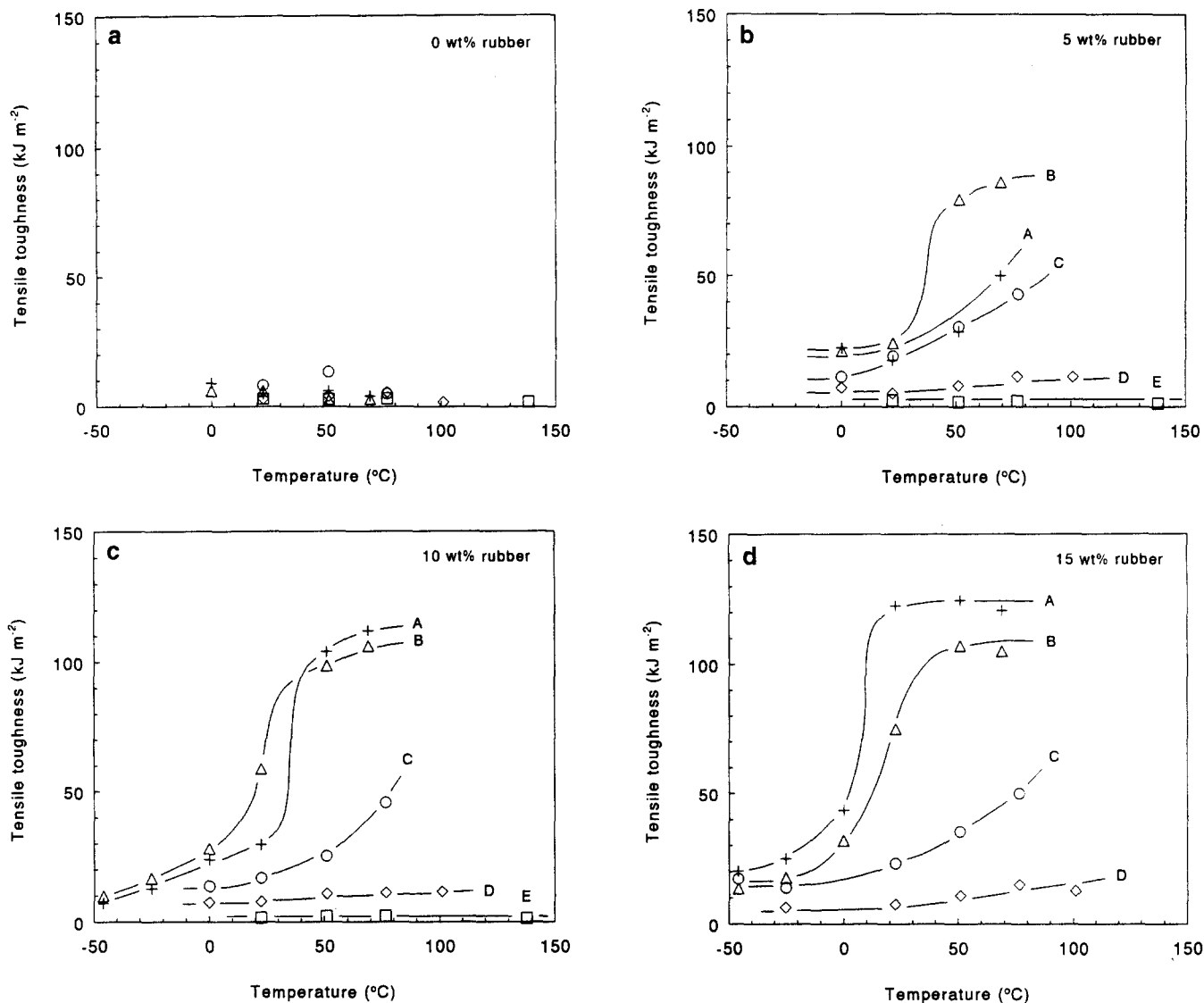


Figure 7 Notched tensile toughness (G_n) of neat and core-shell rubber-modified epoxides versus temperature as a function of the epoxide molecular weight between crosslinks: M_c = (A) 6.79; (B) 4.38; (C) 1.64; (D) 0.88; (E) 0.26 kg mol^{-1} . (a) 0 wt% rubber; (b) 5 wt% rubber; (c) 10 wt% rubber; (d) 15 wt% rubber

Obviously, the maximum degree of ductility is obtained for this epoxide in the tough region. The shift of T_{BT} to lower temperatures because of the increased rubber concentration confirms that the brittle-to-ductile transition is independent of the glass transition of the matrix^{13,14}. The level of tensile toughness of the epoxide corresponding to curve A is increased considerably ($\approx 20 \text{ kJ m}^{-2}$) because of the decrease in ligament thickness (compare curve A in Figures 7c and 7d). Hence, this epoxide with the highest M_c also possesses the highest degree of ductility confirming the conclusions made during the discussion of the slow-speed uniaxial tensile testing and the (slow-speed) fracture toughness measurements. In the literature¹⁴⁻¹⁶, several studies reported a maximum toughness value at a certain crosslink density for neat and rubber-modified epoxides; however, the authors did not realize the importance of the ID_c . Conclusions with respect to the M_c dependency of toughness can only be made if the polymer under investigation is toughened to its maximum extent.

In Figure 8 the recorded force-time traces of two rubber-modified epoxides (5 wt% rubber: $M_c = 0.26$ and 4.38 kg mol^{-1}) are shown measured at 70°C during a notched high-speed tensile test. The striking difference

between the G_n values for these two epoxides (curve A: 5 kJ m^{-2} and curve B: 85 kJ m^{-2}) is elucidated in this figure; the maximum force as well as the strain to break differs considerably for A and B. For the densely crosslinked epoxide (curve A) a brittle fracture is observed; the material is already broken in the elastic region. The fracture process of the less densely crosslinked epoxide (curve B) clearly corresponds to a ductile failure; after the elastic region a true ductile deformation behaviour occurs indicated by the decreasing slope of the force-time trace which even becomes negative at higher strains.

Optical microscopy

In Figure 9 optical micrographs are shown of several high-speed fractured rubber-toughened epoxides (neat epoxides do not show a whitened region and are therefore not analysed).

The micrographs reveal whitened areas below the fracture surface. Whitening is the result of void formation (particle-matrix interface detachment) and/or deformation¹⁷⁻²¹. All the micrographs shown in Figure 9 are taken from fractured samples measured at 70°C as a reference temperature. Micrographs

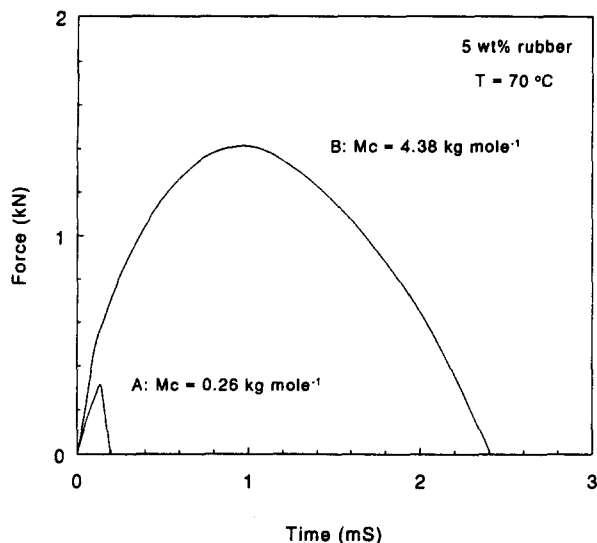


Figure 8 Force-time traces of rubber-modified epoxides recorded at 70°C

corresponding to the epoxides coded as A, B, C and D (see Table 4) are shown in Figures 9d, 9c, 9b and 9a, respectively (all 10 wt% rubber). Clearly, an increase in M_c results in an increase in the whitened volume. Qualitatively, the whitened volume corresponds to the G_h value as given in Figure 7c (70°C).

Critical ligament thickness

In Figure 10 a cross-section of Figure 7 at room temperature is shown, yielding the values of G_h as a function of the core-shell rubber concentration. The brittle-to-ductile transition of the epoxides corresponding to curves C and D is located between 0 and 5 wt% core-shell rubber, hence the corresponding ID_c is positioned above $0.35 \mu\text{m}$ for the given testing conditions and cannot be determined accurately. For the epoxides having an M_c of 4.38 (curve B) and 6.79 kg mol^{-1} (curve A), the brittle-to-ductile transition is located between 5 and 10 wt% rubber, and between 10 and 15 wt% rubber, respectively. If a body-centred lattice is assumed and the average rubber particle diameter is set at $0.2 \mu\text{m}$, the corresponding ID_c can be estimated to be 0.29 and $0.21 \mu\text{m}$, respectively.

In Figure 11 the ID_c values for these two epoxides ($M_c = 4.38$ and 6.79 kg mol^{-1} ; both indicated by a filled circle) are compared with those of the thermoplastic PS-PPE system (indicated by the open circles) as discussed in part 2 of this series².

Although the data of the thermosetting system are determined during notched high-speed tensile measurements, the order of magnitude of the value of ID_c is the same as the values displayed for the thermoplastic system determined during slow-speed uniaxial tensile testing. Moreover, there is some overlap between the values of ID_c for both systems at a network density of $9 \times 10^{25} \text{ chains m}^{-3}$.

The drawn line in Figure 11 indicated by $\sigma_y = 70 \text{ MPa}$ is according to the simple, first-order model presented in part 2², assuming a constant value of the yield stress of 70 MPa. Clearly, the model predictions agree closely with the experimental values despite the simplicity of the model. It is worth noting that the model predictions even seem to be valid for high-speed tensile testing indicating

the insensitivity of the value of ID_c to the testing speed applied. The testing speed and temperature dependency of the ID_c can be understood in terms of the strain rate and temperature dependency of the yield stress, σ_y (see equation (3)). Increasing the strain rate and/or decreasing the testing temperature results in a decrease in the ID_c via an increased σ_y of the matrix material. The σ_y -sensitivity of the ID_c is shown in Figure 11; three different lines are drawn corresponding to the model predictions of ID_c assuming different values for σ_y . From the slow-speed fracture toughness data it could be inferred that the value of ID_c for the epoxides coded A and B was positioned above $0.35 \mu\text{m}$. High-speed tensile testing, however, resulted in values of ID_c of 0.21 and $0.29 \mu\text{m}$, respectively. The lower values of ID_c determined during a high-speed test can be explained in terms of the strain rate dependency of σ_y . In a forthcoming paper¹⁰, the influence of temperature (and testing speed) on the value of ID_c will be discussed more extensively.

In Figure 12 the ID_c is plotted versus the network density on a different scale, allowing for the incorporation of the ID_c of polycarbonate (PC; determined by a notched Izod impact test²³).

The comparison of PC with the other systems displayed in Figure 12 is of interest since PC represents one of the most densely entangled thermoplastic polymers, having an ID_c of approximately $3 \mu\text{m}$. The values of ID_c for thermosetting polymers possessing network densities in the range 15×10^{25} – $235 \times 10^{25} \text{ chains m}^{-3}$ are not incorporated in Figure 12 since it was impossible to determine the value of ID_c using rubbery particles having a diameter of $0.2 \mu\text{m}$ (in this study the same core-shell rubber was used in all systems investigated in order to eliminate the influence of rubber type and particle size). Nevertheless, the prediction of the ID_c for these densely crosslinked polymers (coded C, D and E) can be estimated to be in the range 1–10 μm , indicating that the maximum level of toughness is already obtained after adding just a few per cent (non-adhering) rubbery particles. The absolute value of toughness for these densely crosslinked epoxides, however, will be rather low (see Figures 3 and 10). Extrapolation (dashed line) to the usually applied highly crosslinked epoxides (with a crosslink density around $200 \times 10^{25} \text{ chains m}^{-3}$) indicates that not much can be expected from rubber modification, since the ID_c is to be of the order of a few micrometres. These aspects are the subject of current research at our laboratory. The drawn line in Figure 12 is according to the simple model assuming a constant value of the yield stress of 70 MPa. The model prediction of the ID_c levels off at high values of the network density and starts to deviate from the experimental trend. This is possibly due to an overestimation of the elastic energy available to generate a brittle fracture. Only a more detailed numerical analysis in a rather large area around the strain localization will probably give conclusive answers concerning this aspect. This is currently one of the topics of study in our laboratory.

CONCLUSIONS

Three series of tests were performed on neat and rubber-toughened epoxides: slow-speed tensile testing, slow-speed fracture toughness (G_{Ic}) testing and notched high-speed tensile toughness (G_h) testing. The maximum strain to break of rubber-toughened epoxides (containing

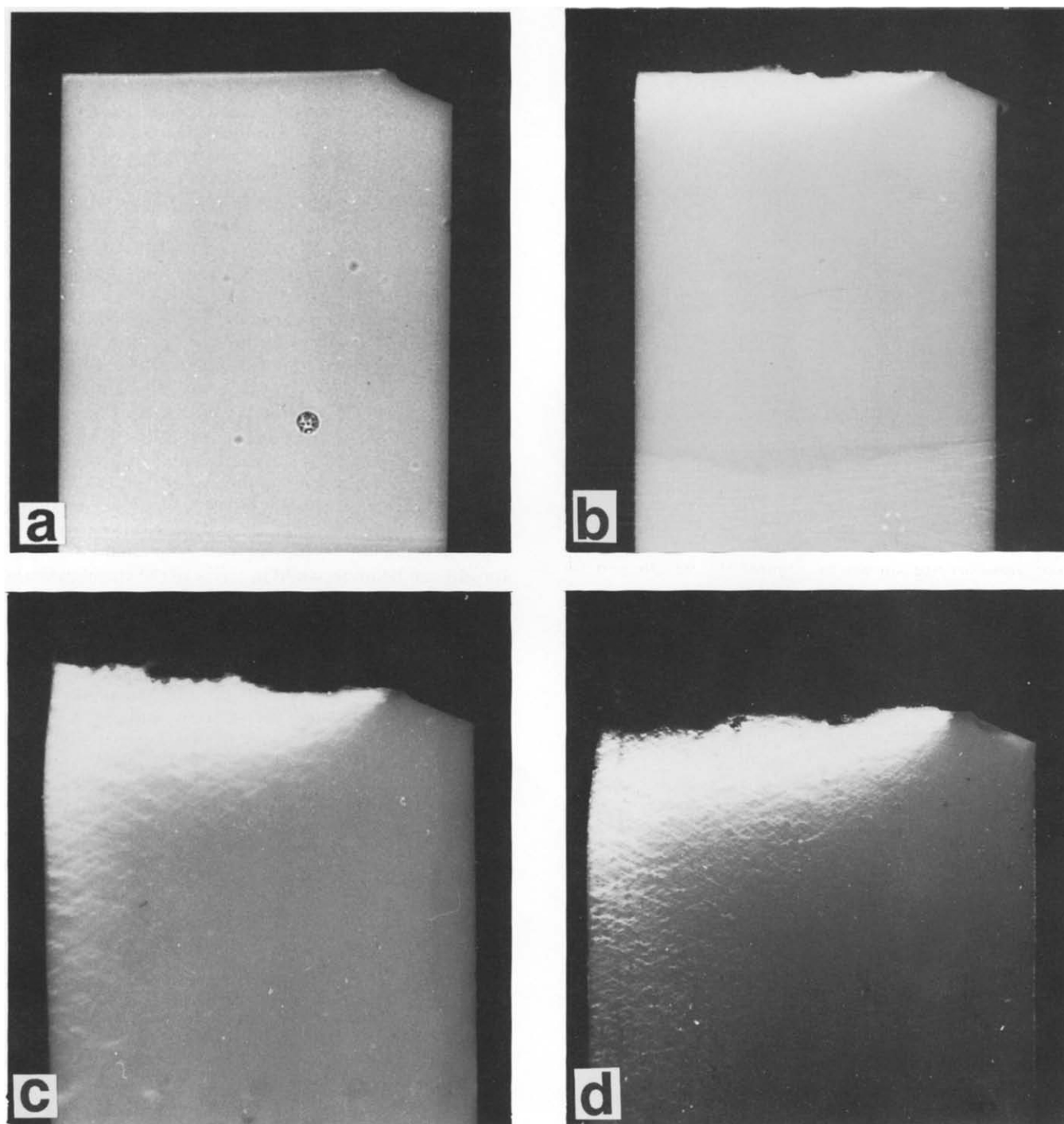


Figure 9 Optical micrographs of high-speed fractured core-shell rubber-modified epoxides (10 wt%); M_c = (a) 0.88; (b) 1.64; (c) 4.38; (d) 6.79 kg mol⁻¹ (reference temperature 70°C)

non-adhering core-shell particles) increases with an increasing molecular weight between crosslinks from 12% ($M_c = 0.88$ kg mol⁻¹) up to 70% ($M_c = 6.79$ kg mol⁻¹) independent of the volume fraction of rubber dispersed in the system. The same deviation between the macroscopic draw ratio (λ_{macro}) and the theoretical draw ratio of a single network strand (λ_{max}), as already observed for the thermoplastic PS-PPE system, is found: $\lambda_{\text{macro}}/\lambda_{\text{max}} = 0.6$. No brittle-to-ductile transition could be observed with slow-speed uniaxial tensile testing.

Slow-speed (10 mm min⁻¹) fracture toughness measurements reveal that the absolute value of G_{Ic} for both neat and rubber-toughened epoxides increases with an increasing value of M_c . For neat epoxides G_{Ic} ranges

from 0.15 kJ m⁻² ($M_c = 0.26$ kg mol⁻¹) to 4.5 kJ m⁻² ($M_c = 6.79$ kg mol⁻¹), while for the rubber-toughened epoxides G_{Ic} varies from 0.4 kJ m⁻² ($M_c = 0.26$ kg mol⁻¹) to 14 kJ m⁻² ($M_c = 6.79$ kg mol⁻¹), independent of the rubber concentration. For all the epoxides investigated ($9 \times 10^{25} \leq v_c \leq 235 \times 10^{25}$ chains m⁻³) in these tests, a brittle-to-ductile transition was observed between 0 and 5 wt% core-shell rubber. Hence, the critical ligament thickness (ID_c) is positioned above 0.35 μm (corresponding to 5 wt% rubber) under these relatively mild testing conditions of a fracture toughness test.

Since the concept of a real ID_c should be valid under all testing conditions applied, notched high-speed tensile testing at various temperatures was carried out. Analogous

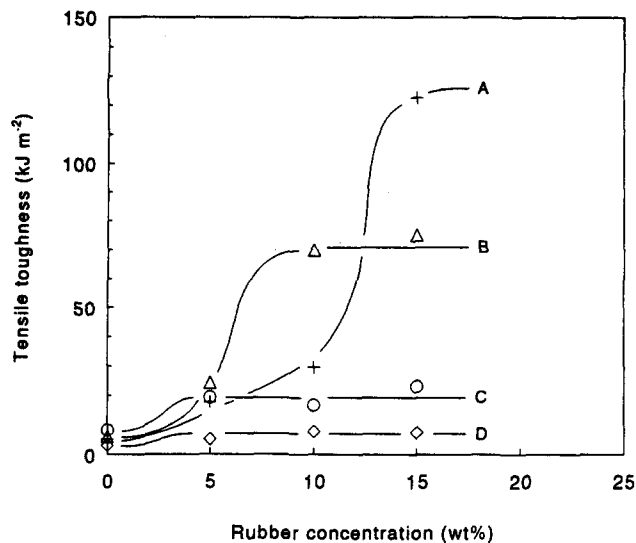


Figure 10 Notched tensile toughness of rubber-modified epoxides versus rubber concentration as a function of the epoxide molecular weight: M_c = (A) 6.79; (B) 4.38; (C) 1.64; (D) 0.88 kg mol⁻¹

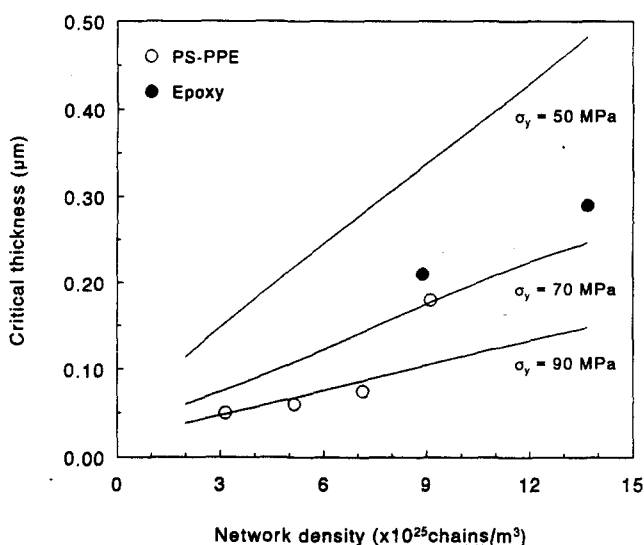


Figure 11 Critical ligament thickness versus network density (entanglement and/or crosslink density). The drawn lines are according to the model. See text for details

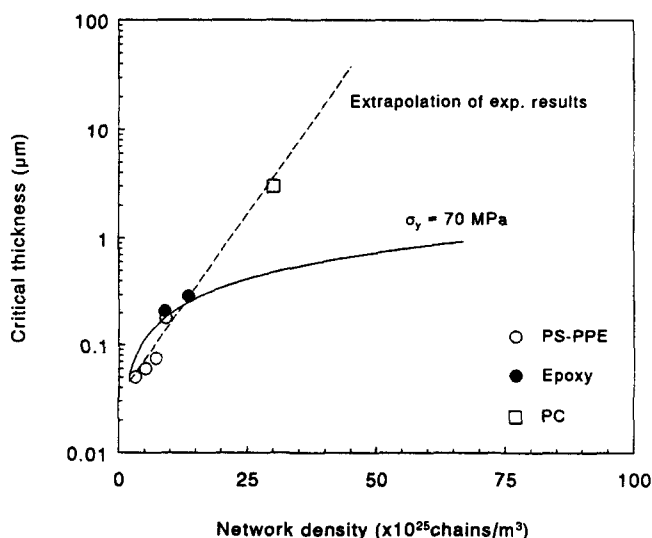


Figure 12 Critical ligament thickness versus network density. The drawn line is according to the model. See text for details

to the results obtained from the slow-speed uniaxial tensile testing and the (slow-speed) fracture toughness measurements, the value of G_b of the rubber-toughened epoxides uniquely increases with increasing M_c : G_b varies from 2 kJ m⁻² ($M_c = 0.26$ kg mol⁻¹) up to 120 kJ m⁻² ($M_c = 6.79$ kg mol⁻¹). The values of ID_c of two relatively loose crosslinked epoxides were determined to be 0.21 μm ($M_c = 6.79$ kg mol⁻¹) and 0.29 μm ($M_c = 4.38$ kg mol⁻¹) under these severe testing conditions at room temperature. The values of ID_c for the more densely crosslinked epoxides could not be determined due to the inaccuracy introduced by the low rubber volume fraction at which the brittle-to-ductile transition occurred. The values of ID_c of the epoxides, determined by notched high-speed tensile testing, correlate well with the values shown in our previous paper for the thermoplastic PS-PPE model system determined by slow-speed uniaxial tensile testing clearly indicating the relative insensitivity of the real ID_c to the testing conditions applied and the nature of the network loci (physical entanglements and/or chemical crosslinks). The experimentally derived values of the ID_c correlate well with the values predicted by the simple first-order model presented in our previous paper². The slight dependency of the ID_c on the testing conditions applied can be understood in terms of the strain rate and temperature dependency of the yield stress.

ACKNOWLEDGEMENTS

The authors are grateful to R. G. M. Schulkes for performing the sample preparation and for carrying out the mechanical analysis of the various epoxides. Mr E. Verhaert (Rohm and Haas Benelux NV, Antwerp, Belgium) is thanked for supplying the core-shell rubber. The research was financed by the Foundation Polymer Blends (SPB).

REFERENCES

- 1 Van der Sanden, M. C. M., Meijer, H. E. H. and Lemstra, P. J. *Polymer* 1993, **34**, 2148
- 2 Van der Sanden, M. C. M., Meijer, H. E. H. and Tervoort, T. A. *Polymer* 1993, **34**, 2961
- 3 Treloar, L. R. G. 'The Physics of Rubber Elasticity', Clarendon, Oxford, 1975
- 4 Kramer, E. J. and Berger, L. L. *Adv. Polym. Sci.* 1990, **91/92**, 1
- 5 Ferry, J. D. 'Viscoelastic Properties of Polymers', John Wiley, New York, 1980
- 6 Nielsen, L. E. *Rev. Makromol. Chem.* 1969, **C3** (1), 77
- 7 Bellenger, V., Verdu, J. and Morel, E. *J. Polym. Sci.* 1987, **B25**, 1219
- 8 Williams, J. G. and Cawood, M. J. *Polym. Testing* 1990, **9**, 15
- 9 Glad, M. D. and Kramer, E. J. *J. Mater. Sci.* 1991, **26**, 2273
- 10 Van der Sanden, M. C. M. and Meijer, H. E. H. *Polymer* submitted
- 11 Pearson, R. A. and Yee, A. F. *J. Mater. Sci.* 1989, **24**, 2571
- 12 Wu, S. *Polymer* 1985, **26**, 1855
- 13 Borggreve, R. J. M. *PhD Thesis* Twente University of Technology, The Netherlands, 1988
- 14 Borggreve, R. J. M., Gaymans, R. J., Schuijjer, J. and Ingen Housz, J. F. *Polymer* 1987, **28**, 1489
- 15 Murakami, S. *et al. Proc. 34th Int. SAMPE Symp.* 1989, p. 2194
- 16 Bell, J. P. *J. Appl. Polym. Sci.* 1970, **14**, 1901
- 17 Garg, A. C. and Mai, Y.-W. *Compos. Sci. Technol.* 1988, **31**, 179
- 18 Kinloch, A. J. and Young, R. J. 'Fracture Behaviour of Polymers', Elsevier, London, 1985
- 19 Parker, D. S., Sue, H. J., Huang, J. and Yee, A. F. *Polymer* 1990, **31**, 2267
- 20 Pearson, R. A. and Yee, A. F. *J. Mater. Sci.* 1986, **21**, 2475
- 21 Bucknall, C. B. 'Toughened Plastics', Applied Science Publishers, London, 1977
- 22 Li, D., Li, X. and Yee, A. F. *Polym. Mater. Sci. Eng.* 1990, **63**, 296
- 23 Wu, S. *Polym. Eng. Sci.* 1990, **30** (13), 753